THE JOURNAL OF PHYSICAL CHEMISTRY A

pubs.acs.org/JPCA

Article

How Many Pnicogen Bonds can be Formed to a Central Atom Simultaneously?

Rafał Wysokiński,* Wiktor Zierkiewicz, Mariusz Michalczyk, and Steve Scheiner*

Cite This: *J. Phys. Chem. A* 2020, 124, 2046–2056

Read Online

ACCESS | Metrics & More | Article Recommendations | Supporting Information

ABSTRACT: A central ZF_3 molecule (Z = P, As, Sb, Bi) is allowed to interact with a number of nucleophiles exemplified by NCH, NH_3, and NC^- anion. The Z···N pnicogen bond (ZB) to a single base grows stronger for heavier Z atom: P < A < Sb < Bi and follows the NCH < NH_3 < NC^- order for the three bases. The maximum number of ZBs depends on both the nature of the base and pnicogen atom. PF_3 and AsF_3 can pnicogen bond with only a single CN^-; SbF_3 and BiF_3 can interact with two anions but only weakly. The weak NCH nucleophile can engage in a maximum of two ZBs, while three ZBs occur for NH_3. The latter NH_3 maximum can be extended to four ZBs but only for BiF_3. The fourth ZB is somewhat longer and weaker than the others, and the entire $(H_3N)_4$···BiF_3 complex relies partially on secondary interactions for its stability.

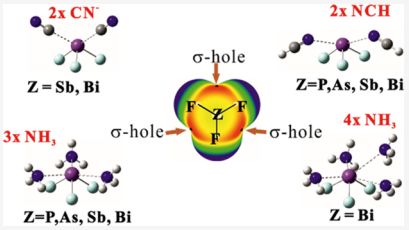

INTRODUCTION

In the years following its initial conception, the hydrogen bond (HB) has become one of the most important and far-reaching phenomena for both chemistry and biology.[1−8] Recent years have witnessed the growth of study of a set of parallel sorts of interactions, replacing the bridging proton of the HB by any set of other elements in the p-block of the periodic table. These electronegative elements are able to attract an electron donor by way of a region of depleted electron density on their periphery, which in turn are commonly referred to as σ- or π-holes.[9−18] A good deal of work has addressed the factors that contribute to this bonding phenomenon, the strength of the interaction, and the subsidiary part played by monomer deformation, to amplify its role in biological systems, pharmacology, and technology.[1,2,19−30] For example, it is now understood that these noncovalent bonds are stabilized by contributions from charge transfer, polarization, and dispersion, in addition to the electrostatic attraction.

Recent work has described a dual scheme, via either σ- or π-hole, by which a base might bind to the tetrel[31,32] or pnicogen[33] atom of a Lewis acid. As one relevant example, the NH_3 base can interact with a substituted $TF_3C_6H_2R_3$ (T = C, Si Ge, Sn, Pb; R = H, CH_3, F) acid through either its axial or equatorial σ-hole, with respect to the phenyl ring.[34] Likewise, a substituted pyridine base engages in a tetrel bond with the central T atom of TF_4 by first distorting the latter into a trigonal bipyramid arrangement, after which both the axial and equatorial site σ-holes are open to attack.[32] A pair of incoming bases can interact with either the σ or π-holes surrounding a TF_4 molecule,[31] wherein the existence of π-holes depends upon a prior distortion of the tetrahedral TF_4 to a planar configuration.

Moreover, in connection with the latter idea of the presence of multiple noncovalent bonds there is indeed growing interest concerning the clustering of molecules, for instance $(PH_2F)_n$, $(PH_2Cl)_n$,[35] NH_3, PH_3, and PFH_2[36] and HF, FCl,[37−52] wherein such multiple bonds are integral. It has long been recognized that the formation of a HB polarizes each participant and affects their ability to engage in a second such bond. For example, the formation of a AH···BH dimer shifts electron density from BH to AH, making the former a better electron donor. The addition of a third CH molecule to the growing chain can take advantage of this charge shift so that AH···BH···CH is bound by more than the simple sum of the AH···BH and BH···CH bond energies within these respective dimers, a phenomenon known as positive cooperativity. A second factor takes on added importance in the case of certain other noncovalent bonds. The formation of a tetrel bond, for instance, can drastically alter the internal geometry of the Lewis acid. This nuclear rearrangement in turn exerts a very strong influence upon the electrostatic potential surrounding it, which in turn can enhance or inhibit its ability to engage in a second such bond.

The earlier work cited above has documented the ability of the central tetrel atom to engage in two noncovalent interactions simultaneously. Very recent calculations have noted that the hypervalent YF_4 (Y = S, Se, Te, Po) can similarly engage in a pair of chalcogen bonds.[53] Two NCH molecules can form a pair of tetrel bonds to a central TF_4 molecule (T = Si, Ge, Sn, Pb).[31,54−56]

Received: January 10, 2020
Revised: February 13, 2020
Published: February 13, 2020

https://dx.doi.org/10.1021/acs.jpca.0c00257
J. Phys. Chem. A 2020, 124, 2046–2056

These earlier findings lead to the natural question as to just how many nucleophiles can be attached to a Lewis acid at the same time. What is the maximum number of such bonds that can be present, and how does this number differ for tetrel, pnicogen, and chalcogen bonds? Surely there will be a point at which simple issues of steric strain will prevent any further bases from approaching. Just how much can the central molecule alter its structure so as to accommodate additional bonds? How might this maximum number depend on the precise nature of the Lewis acid and base molecules? Another issue relates to cooperativity. Does the presence of the first bond strengthen or weaken the second and so on? Does this cooperativity operate through simple electronic polarization or does geometric deformation play an important role?

As a vehicle to begin to answer some of these questions, the work described below considers the pnicogen bonds (ZBs) that might be formed by ZF_3 (Z = P, As, Sb, Bi). As guidance in terms of the formal definition of a pnicogen bond, we employ the IUPAC definitions[57,58] that have been developed for the very similar halogen and chalcogen bonds. These bonds are characterized[59] by the approach to a pnicogen atom, acting as a Lewis acid, of a nucleophile, which are built upon electrostatic attraction, polarization, and dispersion.

Three different bases are considered. Neutral HCN can engage in a ZB through its N atom, whereas the negative charge on CN^- will naturally lead to a much stronger interaction. This anion also presents the interesting question as to whether it will interact with the Z through its C or N atom; in fact, it is also possible in principle that the negative potential above the CN axis could play the role of the electron donor as well. NH_3 represents an intermediate case. Like HCN, NH_3 is also a neutral molecule so is a weaker nucleophile than CN^-, but its sp^3 hybridization makes it stronger than HCN. One, then two, three, and four base units are added sequentially to the ZF_3 molecule, so as to determine how many ZBs are possible for each combination of ZF_3 and base. At the same time, the properties of each complex are monitored to follow changes occurring in each system upon each addition of another base unit.

METHODS

The geometries of isolated ZF_3 (Z = P, As, Sb, Bi), NH_3 and HCN molecules, and CN^- anion as well as their ZF_3L_n complexes (L = HCN and CN^-, where n = 1−3) were fully optimized at the MP2 level of theory with the aug-cc-pVDZ basis set.[60,61] This level of theory has been found to be consistent with CCSD(T) with larger basis sets and with available experimental quantities, for complexes stabilized by noncovalent forces.[62−65] Pseudopotentials which include relativistic effects were used for the heavy Sb and Bi atoms.[66] The absence of any imaginary frequency guaranteed that the generated structures are true minima. Energies were also computed at the CCSD(T)/aug-cc-pVDZ level (using MP2 minima) for purposes of comparison and validation.[67−73] Interaction energies were calculated as the difference in energy between the complex and the sum of monomers (with the same geometries as they adopt within the complex). Binding energies were computed relative to the monomers in their isolated optimized structures. Both quantities were corrected for basis set superposition error (BSSE) using the counterpoise protocol.[74]

All computations were performed via the Gaussian 16 software package.[75] Molecular electrostatic potential (MEP) analysis was applied to identify and quantify MEP extrema using the WFA-SAS[76] and MultiWFN programs.[77,78] The electron density topology was analyzed using AIMAll software.[79] In order to analyze interorbital connections and charge flow between the monomers, the natural bond orbital (NBO) procedure (using GenNBO 6.0) was utilized using the wavefunction generated at the DFT level for MP2 geometries.[80] The CSD (Cambridge Structural Database, CCDC 2019, ConQuest ver. 2.0.1)[81] was searched for pertinent experimental crystal structures similar to those described here.

RESULTS

Monomers. The ZF_3 (Z = P, As, Sb, Bi) monomers as well as HCN, NH_3, and CN^- anion were fully optimized at the MP2/aug-cc-pVDZ level of theory. All ZF_3 molecules have a pyramidal C_{3v} structure with a pnicogen Z atom at the apex and three F atoms in the base. As may be seen in the details of these structures in Table S1, the Z−F bond length increases as the Z atom grows in size from 1.630 for PF_3 to 2.016 in BiF_3. The sum of the three θ(F−Z−F) angles in the last column of Table S1 decreases slightly with larger Z, indicating a less planar geometry.

The MEP of each ZF_3 molecule has a similar profile, exemplified in Figure 1 for AsF_3. Each F atom is surrounded by a blue negative region, while a red positive area termed a σ-hole lies opposite each Z−F bond. There is another positive region, but a much less intense one, that lies opposite the Z lone pair, amongst the three F atoms. For lack of a better name, and for convenience in discussion, this latter point is designated as a π-hole here, although the reader must be aware that the ZF_3 molecule is not flat and does not contain a π-electron system per se. The values of $V_{s,max}$ for these σ and π-holes are listed in the upper portion of Table 1, which shows the expected trend of a more intense positive region for larger Z atoms (with a small irregularity between P and As for the π-holes). The HCN molecule contains a minimum in its MEP on its N atom along the molecular axis, with a $V_{s,min}$ value of −31.4 kcal/mol, as seen in the lower part of Table 1. The MEP minimum of NH_3 is along its C_3 axis, coincident with its lone pair. Its value is a bit more negative than that of HCN. Because of its negative charge, the MEP of CN^- is much more negative with minima of roughly equivalent intensities on the N and C atoms, as well as along the anion's equator, its π-region.

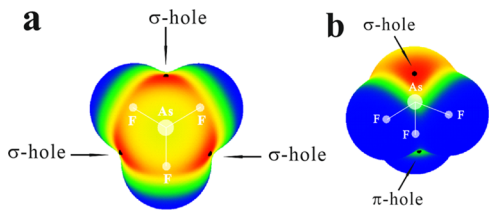

Figure 1. MEP on the 0.001 au isodensity surface at the MP2/cc-pVDZ level of AsF_3 (a, top view and b, bottom view) isolated monomers. Color ranges, in kcal/mol, are red greater than 35, yellow between 15 and 35, green between 0 and 15, and blue below 0 kcal/mol.

ZF_3 + 1 Base. The structures of the most stable complexes arising from the addition of a single base to ZF_3 are presented in Figure 2. The neutral HCN approaches N-atom first, toward one of the σ-holes of ZF_3, opposite the F atom labeled F1. As observed in the first column of Table 2, the intermolecular

https://dx.doi.org/10.1021/acs.jpca.0c00257
J. Phys. Chem. A 2020, 124, 2046−2056

Table 1. MEP Maxima (kcal/mol) on the 0.001 au Isodensity Surface of ZF_3 (Z = P, As, Sb, Bi) and HCN and CN^- Monomers, Calculated at the MP2/aug-cc-pVDZ Level of Theory

molecule	$V_{S,max}$ (Z-F) σ-hole	$V_{S,max}$ π-hole below Z atom
PF_3	35.6	9.7
AsF_3	43.9	7.1
SbF_3	51.6	10.6
BiF_3	61.5	12.7
molecule		$V_{s,min}$
HCN		−31.4
NH_3		−37.7
CN^-		−137.7 (N) π
		−136.6 (N)
		−135.5(C)

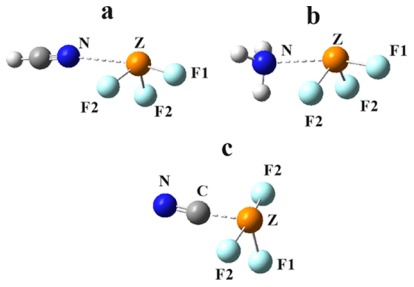

Figure 2. Most stable conformers of HCN, NH_3, and CN^- with ZF_3.

separation R(N···Z) becomes shorter as Z grows larger, despite the increasing van der Waals (vdW) radius of this Z atom. Due in part to the normal transfer of charge from the base lone pair into the σ^*(Z−F1) antibonding orbital, r(Z−F1) is consistently the longest bond within the ZF_3 molecule, by between 0.008 and 0.0121 Å. Consistent with the trend of a pnicogen bond toward linearity, the θ(N···Z−F1) angles lie in the 163−171° range. The next column of Table 2 indicates the level of nonplanarity in the ZF_3 subunit, followed by the decrease relative to the unperturbed monomer in the last column. The negative values of $\Delta\Sigma\theta$ indicate a more pyramidal structure within the dimer. Many of the same trends are seen in the complexes with NH_3 in the next section of Table 2, but the data suggest a stronger interaction. The intermolecular R(N···Z) distances are considerably shorter, in the 2.6−2.8 Å range, and the internal r(Z−F) stretches are of larger magnitude; again r(Z−F1) is longer than r(Z−F2). The θ(N···Z−F1) angles are a bit less linear, but the $\Sigma\theta$ angle sums are a bit smaller, indicating somewhat more pyramidality induced within ZF_3.

The lowest section of Table 2 lists the same properties for the complexes with the CN^- anion. Importantly, the structures of these complexes are rather different than those with the neutral bases. As seen in Figure 2c, the ZF_3 molecule becomes very nearly planar. This approach to planarity is evident in the last two columns of Table 2 where the sum of the three θ(F−Z−F) angles grows by 50−60° up to nearly 360°. The full charge on this base leads to much shorter intermolecular distances, around 2 Å. In addition, the trend in R(C···Z) is opposite that for the complexes with neutral HCN in that the separation increases as the Z atom grows in size. The stronger binding to the anion is also exemplified by the much longer internal r(Z−F) distances.

The binding energies of these complexes, corresponding to the reaction that forms the dimer from the pair of isolated monomers, displayed in the first two columns of Table 3, reaffirms the indications of the binding strength arising from Table 2. Whereas HCN binds with an energy between 3 and 7 kcal/mol, dimers involving NH_3 are bound by 4.5−13 kcal/mol, and the anion range is considerably larger, 23−39 kcal/mol. In all cases, the binding is enhanced for larger Z atoms. The interaction energies in the next two columns of Table 3 refer to the pure interaction between the monomers which have already been deformed into the geometries they adopt within the complex. As such E_{int} is more negative than E_b, differing by a deformation energy E_{def} which is needed to distort each monomer appropriately. There is little deformation involved in the complexation with the neutral bases. However, the large distortion of ZF_3 from its pyramidal structure when complexed with the anion leads to much more negative interaction energies in the bottom segment of Table 3. These deformation energies are the largest for the smaller Z atoms, with E_{def} rising from 33.9 kcal/mol for BiF_3 up to 55.0

Table 2. Structural Parameters (Distances in Å, Angles in Degs) in Complexes of ZF_3 Plus One Base, Calculated at the MP2/aug-cc-pVDZ Level of Theory

	R(N···Z)	r(Z−F1)	r(Z−F2)	θ(N···Z−F1)	$\Sigma\theta$(F−Z−F)	$\Delta\Sigma\theta$
			HCN···ZF_3			
HCN···PF_3	3.032	1.639	1.631	171.3	289.5	−1.7
HCN···AsF_3	2.907	1.758	1.749	169.5	285.4	−2.8
HCN···SbF_3	2.864	1.933	1.923	162.6	280.6	−3.9
HCN···BiF_3	2.860	2.035	2.023	165.5	283.0	−3.6
			H_3N···ZF_3			
H_3N···PF_3	2.780	1.647	1.638	168.5	287.2	−4.0
H_3N···AsF_3	2.593	1.771	1.759	164.1	282.1	−6.1
H_3N···SbF_3	2.592	1.945	1.937	155.5	277.0	−7.5
H_3N···BiF_3	2.670	2.045	2.035	155.4	279.6	−7.0
	R(C···Z)	r(Z−F1)	r(Z−F2)	θ(C···Z−F1/2)	$\Sigma\theta$(F−Z−F)	$\Delta\Sigma\theta$
			NC^-···ZF_3			
NC^-···PF_3	1.863	1.675	1.805	99.3/85.0	341.7	50.5
NC^-···AsF_3	1.978	1.785	1.907	98.0/84.3	339.4	51.2
NC^-···SbF_3	2.187	1.951	2.046	98.4/82.6	331.7	47.2
NC^-···BiF_3	2.285	2.049	2.166	89.6/84.5	347.9	61.3

https://dx.doi.org/10.1021/acs.jpca.0c00257
J. Phys. Chem. A 2020, 124, 2046−2056

Table 3. Binding (E_b) and Interaction Energies (E_{int}) (kcal/mol) of ZF_3 Complexes with HCN and CN^- Calculated at the MP2/aug-cc-pVDZ (I) and CCSD(T)/aug-cc-pVDZ (II) Levels of Theory[a]

	E_b		E_{int}	
	(I)	(II)	(I)	(II)
		HCN···ZF_3		
HCN···PF_3	−2.74	−2.51	−2.82	−2.54
HCN···AsF_3	−4.09	−3.72	−4.24	−3.80
HCN···SbF_3	−5.88	−5.35	−6.15	−5.53
HCN···BiF_3	−7.48	−6.95	−7.75	−7.14
		H_3N···ZF_3		
H_3N···PF_3	−4.45	−4.40	−4.87	−4.75
H_3N···AsF_3	−7.32	−7.05	−8.24	−7.90
H_3N···SbF_3	−11.70	−11.35	−13.09	−12.71
H_3N···BiF_3	−13.20	−12.92	−14.31	−13.99
		NC^-···ZF_3		
NC^-···PF_3	−22.68	−20.00	−77.66	−74.64
NC^-···AsF_3	−30.93	−28.44	−77.79	−75.06
NC^-···SbF_3	−38.67	−36.70	−74.72	−72.36
NC^-···BiF_3	−39.24	−37.41	−73.16	−70.74

[a]All values corrected for BSSE.

kcal/mol for PF_3, as reported in Table S2. While E_b and E_{int} obey similar trends for the neutral bases which involve only small deformation energies, there is a reversal for the anion. The binding energies of the $NC^-\cdots ZF_3$ complexes rise steadily for the P < As < Sb < Bi sequence, but there is no such increase for E_{int}, which in fact shows a small decrease. It should be mentioned finally that these energetics are not very sensitive to the means of incorporating electron correlation. The CCSD(T) quantities in Table 3 are rather similar to the MP2 values, and all trends are identical.

The AIM diagrams of all of these complexes contain a bond path between the Z and N/C atoms involved in the interaction. The relevant properties of the bond critical point are displayed in Table S3 and reflect the energetics fairly well. For example, the density at this critical point for the two neutral bases rises regularly as the Z atom is enlarged from P to Bi, although there is a small dip from Sb to Bi; $\nabla^2\rho$ undergoes a similar increase. Just as the interaction energies of the complexes with CN^- diminish with larger Z atom, so do the values of ρ_{BCP}, although the Laplacian changes are less consistent.

There are also secondary minima for the dimers discussed above. In the case of HCN, this neutral molecule can approach along the C_3 axis, directly opposite the Z lone pair, facilitated by a shallow π-hole in this region. Such a structure is less stable than the σ-hole geometries by the following amounts: 3.6, 5.7, 7.6, and 9.0 kcal/mol for the P, As, Sb, Bi series, respectively. In fact, after correction for BSSE, these alternative structures are barely bound at all, with positive interaction and binding energies. NH_3 can also engage in a similar sort of complex, approaching opposite the Z lone pair, but these structures are quite a bit higher in energy and only those with SbF_3 and BiF_3 are bound after counterpoise correction.

The complexes with the anion have three alternative secondary minima. In addition to the global minimum A in Figure S1, another minimum B occurs when the anion approaches along a σ-hole of ZF_3, causing a lesser degree of deformation. According to Table S4, this structure lies some 1.5−4 kcal/mol higher in energy than A. In configurations C and D, it is the N atom of CN^- that approaches Z rather than C. If the anion approaches a σ-hole, structure C is less stable than A by 2−6 kcal/mol, but this margin rises to the 8−12 kcal/mol level when approaching the π-hole as in D. The energetic edge of geometry A is the smallest for the largest Z atom Bi, where for example, the A conformer involving the σ-hole is more stable than the B π-hole approach by only 1.5 kcal/mol. As one would expect from the diagrams, the transformation of the ZF_3 geometry to a nearly planar configuration structure D leads to high deformation energies as were noted for A, with these values in the 33−53 kcal/mol range reported in Table S5. The less extensive rearrangement within structures B and C leads to much smaller deformation energies, of 11 kcal/mol or less.

Some of these trends would not be easily predictable from a purely electrostatic standpoint, referring to the MEP of each subunit. In the first place, there is little to differentiate the C and N ends of CN^- in terms of $V_{s,min}$, as documented in Table 1, so the strong preference for the C end might appear surprising. However, more to the point, the σ-hole of each ZF_3 molecule is far more intense than its π-hole which is at odds with the dominance of the A structure. This preference for the π-hole geometry of the $F_3Z\cdots CN^-$ dimers is particularly notable in that this sort of geometry must overcome a very large deformation energy involved in the rearrangement of the F_3Z unit, indicated above.

MEP diagrams were generated for various dimers, as pertinent to the next step involving addition of a second base. These complexes retain a σ-hole that lies opposite each F2−Z bond, that is, those not occupied by a base. However, the charge transferred from the base to ZF_3 reduces the magnitude of the remaining σ-holes. The values of $V_{s,max}$ for each of these dimers are provided in Table S6. They remain positive for both neutral bases but are reduced in magnitude by some 11−15 kcal/mol by NCH and by 14−18 kcal/mol for NH_3. The much larger charge transfer from the CN^- anion reverses the previous positive value of $V_{s,max}$, making it negative. The charge transferred, even the smaller amount coming from the neutral bases, causes the shallow π-holes of ZF_3 to all become negative. This characterization of the dimer MEPs would predict that the one involving a CN^- anion ought to be incapable of forming a trimer with a second base and those with the neutral bases retain a positive σ-hole; so the formation of a trimer is a possibility.

ZF_3 + 2 Bases. The addition of another base molecule to each heterotrimer leads to the structures of the trimers in Figure 3. As in the case of the dimers, it is the N atom of HCN

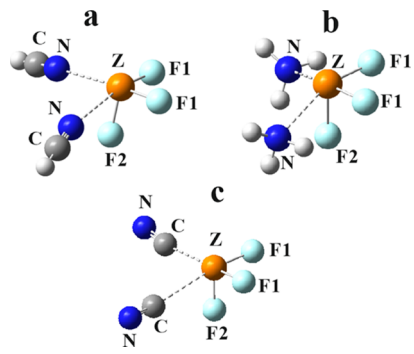

Figure 3. Most stable geometries of trimers including two bases plus ZF_3.

https://dx.doi.org/10.1021/acs.jpca.0c00257
J. Phys. Chem. A 2020, 124, 2046−2056

Table 4. Structural Parameters (Å and Degrees) in $(HCN)_2\cdots ZF_3$ and $(CN)_2\cdots ZF_3$ Complexes at the MP2/aug-cc-pVDZ Level of Theory

	R(N···Z)	r(Z−F1)	r(Z−F2)	θ(N···Z−F1)	$\Sigma\theta$(F−Z−F)
			$(HCN)_2\cdots ZF_3$		
$(HCN)_2\cdots PF_3$	3.076	1.640	1.632	170.5	288.1
$(HCN)_2\cdots AsF_3$	2.968	1.760	1.752	168.4	283.3
$(HCN)_2\cdots SbF_3$	2.940	1.937	1.928	161.2	277.6
$(HCN)_2\cdots BiF_3$	2.905	2.040	2.029	164.1	279.3
			$(H_3N)_2\cdots ZF_3$		
$(H_3N)_2\cdots PF_3$	2.895	1.652	1.643	166.1	284.4
$(H_3N)_2\cdots AsF_3$	2.733	1.780	1.767	162.3	278.0
$(H_3N)_2\cdots SbF_3$	2.688	1.962	1.948	154.1	270.6
$(H_3N)_2\cdots BiF_3$	2.718	2.066	2.049	154.3	273.4
	r(C···Z)	r(Z−F1)	r(Z−F2)	θ(C···Z−F1)	$\Sigma\theta$(F−Z−F)
			$(NC^-)_2\cdots ZF_3$		
$(NC^-)_2\cdots SbF_3$	2.550	2.059	1.957	166.4	259.2
$(NC^-)_2\cdots BiF_3$	2.727	2.164	2.057	177.5	269.1

and NH_3 that approaches the central pnicogen and the C of CN^- in the most stable trimers. The structure of each trimer can be thought of as a distorted octahedron. One apex is occupied by the Z lone pair, and the two ligands lie syn to one another, both directly opposite a F atom, designated F1 in Figure 3. As can be seen by the angles in Table 4, these θ(N/C···ZF1) angles are roughly linear. Note that the intermolecular R(N/C···Z) distances are a bit longer in the trimers than in the corresponding dimers. This stretch amounts to some 0.04−0.08 Å for the HCN trimers and 0.05−0.14 Å for NH_3 but is much longer for the trimers involving the CN^- anion, on the order of 0.4 Å. In fact, for the smaller P and As atoms, there is no trimer of the sort illustrated in Figure 3 for a pair of CN^- anions. This failure to form a trimer is likely due first to the negative values of $V_{s,max}$ for the σ-holes within the $CN^-\cdots ZF_3$ dimers mentioned above. As another consideration, the P and As atoms have fairly small radii, 1.90 and 1.88 Å, respectively, as compared to 2.47 Å for Sb and 2.54 Å for Bi. The short R(C···Z) distances to this anion (see Table 2) result in overcrowding to the smaller Z atoms, coupled with Coulombic repulsion between the two CN^- anions. For illustrative purposes, if the C atoms are each placed 2 Å from Z, roughly equivalent to these lengths in the dimer, and positioned 90° from one another, they would lie only 1.4 Å from one another, inducing obvious strong steric repulsion. It is no wonder then that this distance stretches to more than 2.5 Å for those trimers that can overcome this repulsive effect. The approach of the ZF_3 geometry toward an octahedron is evident by the $\Sigma\theta$(F−Z−F) sums in Table 4 which lie between 260 and 288°; this sum would be 3 × 90° = 270° for a perfect octahedron. However, these angle sums are notably smaller for the NC^- complexes where the F atoms are forced closer together by the short R(Z···C) contacts. The presence of the base opposite each Z−F1 bond elongates this covalent bond even more than in the dimer.

The energetics of formation of these trimers from three separate subunits are compiled in Table 5. As noted above for the dimers, the two separate levels of theory are in good agreement with one another. The addition of a second HCN or NH_3 to form the trimer leads to a significant enhancement of the complexation energies. This magnification is not quite a doubling, lying in the range between 1.6 and 1.9. The situation is quite different for CN^- where the trimer is much more weakly bound. Indeed, the binding energy is positive and only

Table 5. Binding (E_b) and Interaction Energies (E_{int}) (kcal/mol) of ZF_3 Complexes with a Pair of HCN and CN^- Units Calculated at the MP2/aug-cc-pVDZ (I) and CCSD(T)/aug-cc-pVDZ (II) Levels of Theory[a]

	E_b		E_{int}	
	(I)	(II)	(I)	(II)
		$(HCN)_2\cdots ZF_3$		
$(HCN)_2\cdots PF_3$	−4.57	−4.14	−4.70	−4.19
$(HCN)_2\cdots AsF_3$	−7.19	−6.50	−7.51	−6.70
$(HCN)_2\cdots SbF_3$	−10.48	−9.48	−11.06	−9.93
$(HCN)_2\cdots BiF_3$	−13.85	−12.86	−14.57	−13.44
		$(H_3N)_2\cdots PF_3$		
$(H_3N)_2\cdots PF_3$	−7.70	−7.74	−8.66	−8.60
$(H_3N)_2\cdots AsF_3$	−12.90	−12.61	−14.88	−14.49
$(H_3N)_2\cdots SbF_3$	−20.22	−19.68	−23.28	−22.68
$(H_3N)_2\cdots BiF_3$	−24.46	−24.00	−27.45	−26.93
		$(NC^-)_2\cdots ZF_3$		
$(NC^-)_2\cdots SbF_3$	10.80	13.06	−4.29	−1.84
$(NC^-)_2\cdots BiF_3$	−0.63	0.86	−12.92	−11.28

[a]All values corrected for BSSE.

becomes negative when considering the interaction energy. This weak binding of the second anion can be attributed in large part to the Coulombic repulsion between the $NC^-\cdots ZF_3$ anionic complex and the incoming CN^- anion.

Some of these effects are emphasized when considering the various pairwise interaction energies within the trimers. E_1 and E_2 in Table S7 which reference the interaction of each base with ZF_3 are all negative. In the case of the two neutral bases, these quantities are similar to those in Table 3 for the dimers, but they are reduced for the CN^- trimers, consistent with the R(Z···C) bond stretches. Most important are the interaction energies computed between the two bases, within the geometric context of the trimer. These quantities are only very slightly positive, roughly 1 kcal/mol for HCN and NH_3. However, the Coulombic repulsion between the two anions raises E_3 in Table S7 up to more than +70 kcal/mol, severely reducing the total interaction energy within the full trimer. The difference between the total interaction energy and the sum of pairwise interactions represents a measure of the cooperativity within the trimer. While E_{coop} is again only slightly positive for HCN and NH_3, less than 3 kcal/mol, it rises to more than 10 kcal/mol for the anions. In other words, the trimerization

https://dx.doi.org/10.1021/acs.jpca.0c00257
J. Phys. Chem. A 2020, 124, 2046−2056

suffers not only from the pure Coulombic repulsion between the two anions but also by an anticooperative effect.

The various AIM parameters that describe these interactions are displayed in Table S8 where these quantities are again notably larger for the complexes involving the anions than with the neutrals. The bond critical point densities, for example, are in the 0.037−0.047 au range for $(NC^-)_2\cdots ZF_3$ but only 0.011−0.030 for the neutral analogues. While these AIM descriptors are smaller for the anion trimers than for the corresponding anion dimers, their larger magnitudes when compared to the neutral trimers are consistent with the idea that the anions are intrinsically bonded more strongly than the neutrals, but the overall binding energies suffer from the interanionic repulsions.

Anticipating the possibility of adding a third base, the MEP of the various $L_2\cdots ZF_3$ trimers was examined. There is a further erosion of the σ-holes relative to the dimers, caused by the charge transfer from the second base. The values of $V_{s,max}$ contained in Table S9 for the σ-holes are reduced by some 10−17 kcal/mol for the neutral bases, leaving them in the range of only 13−35 kcal/mol. The values for the $(NC^-)_2\cdots ZF_3$ trimers are very negative, between −120 and −147 kcal/mol, which would of course make it exceedingly difficult for these trimers to accept a third anion.

As was the case for the dimers, there are other alternate minima for the trimers as well. For the CN^- trimers, the other configurations look very much like those in Figure 3, except that the approaching atom can be N rather than C (but only for Z = Sb and Bi). There is not much of a distinction between them in terms of energy. For example, flipping one of the two anions around raises the energy by less than 1 kcal/mol. Very much the same is true if both CN^- anions are rotated around to approach via their N atoms. In addition to the $(NH_3)_2\cdots ZF_3$ geometry pictured in Figure 3, there are two alternate minima on the surface (see Figure S2). Whereas the two NH_3 molecules in global minimum A occupy two of the four legs of a tetragonal pyramid, they are located nearly opposite one another in geometry B. The latter is higher in energy than global minimum A by 5−19 kcal/mol. A third structure C is similar to A in that the framework is that of a tetragonal pyramid, except that the NH_3 molecules are located at the vertex and on one leg. This sort of geometry only occurs for the two heavier Z atoms Sb and Bi, for which it is 4−6 kcal/mol higher in energy than A.

More than Two Bases. The situation becomes more varied and interesting upon the addition of a third base to form a tetramer with ZF_3. Three CN^- anions will not engage in a stable complex with a central ZF_3. This failure is likely due to the energetic difficulty of adding yet another anion to a $ZF_3\cdots(CN^-)_2$ complex that already bears a charge of −2. The situation is a bit more nuanced for HCN. Three HCN molecules can form a stable complex with ZF_3, with all positive vibrational frequencies. However, the AIM molecular diagrams in Figure S3 make it clear that only two of the HCN molecules engage in a pnicogen bond with the central Z. For PF_3, the HCN rotates around so that its H participates in a bifurcated H-bond with two F atoms. For the other ZF_3 molecules, the binding is dependent on weak C···F tetrel bonds with the central C of HCN.

It is only NH_3 which can engage in three simultaneous pnicogen bonds with ZF_3. Two views of the structure of these tetramers are displayed in Figure 4, with their corresponding structural parameters in Table 6. Because of the negative cooperativity, the R(N···Z) distances are all a bit longer for the tetramers than for the corresponding trimers. (There is a small amount of asymmetry for PF_3, with three slightly different R(N···P) distances.) There is a further lengthening of the internal Z−F bond lengths, and the pyramidalization of ZF_3 is enhanced relative to the trimers, vis a vis the smaller Σ(F−Z−F) sums.

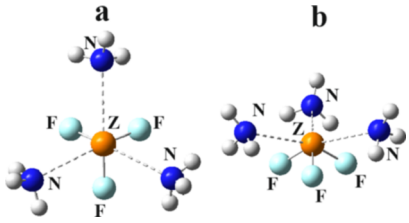

Figure 4. Two views of the optimized structure of $(H_3N)_3\cdots ZF_3$.

The energetics of these tetramers are reported in Table 7. Comparison with the data in Table 5 shows that the total complexation energies are larger than in the trimers. There is a certain degree of negative cooperativity, as these quantities are a bit less than 3/2 as would be expected from simple addition of bond energies. The AIM diagrams of these tetramers in Figure S4 confirm that the binding is indeed due to three Z···N pnicogen bonds, although there are some secondary interactions for Z = Bi. The AIM parameters in Table S10 show an increasing ZB strength with growing Z atom, P < As < Sb < Bi, but each is slightly smaller than the corresponding quantity in the trimer, further evidence of negative cooperativity.

A last issue considered was the question as to whether a ZF_3 molecule could engage in a fourth ZB. It was found that a pentamer of this type could only be formed between 4 NH_3 molecules and BiF_3, the largest Z atom considered. The structure displayed in Figure 5 is not symmetric in that there are four unequal R(Bi···N) distances, varying from 2.65 to 3.14 Å. Moreover, the crowded nature of the complex pushes the θ(F−Bi···N) angles away from linearity. Nevertheless, there are indeed four pnicogen bonds present according to AIM analysis, with bond critical point densities between 0.013 and 0.035 au. On the other hand, Figure S5 indicates that these four ZBs are not the only interactions holding the complex together. They are complemented by a set of a N···F pnicogen bond and NH···F HBs. The entire pentamer is held together with a binding energy of −38.7 kcal/mol. This quantity is only slightly larger than the value in the tetramer of −34.4, so one can conclude that the fourth NH_3 is held by only 4.3 kcal/mol. Given this small amount, which depends not only on the four Bi···N ZBs but also on a number of secondary interactions, the ability of BiF_3 to engage in more than three ZBs is in doubt. In addition, the lighter Z atoms do not show any proclivity whatsoever to form more than three ZBs.

CSD Survey. A survey of previously derived crystals within the CSD[81] (Cambridge Structural Database) provides some experimental context for the computational data above. In order to provide a comprehensive overview, only trivalent ZR_3 units were considered. The samples were divided into those with all three R substituents a halogen (X) atom, and all others separately. N was chosen as the atom of the approaching nucleophile. In order to rule out covalent Z−N bonds and focus on noncovalent pnicogen bonds, a minimum criterion was set for the R(Z···N) interatomic distance. This threshold was taken at three different values: 110, 120, and 130% of the sum of the covalent radii of the Z and N atoms. The maximum

https://dx.doi.org/10.1021/acs.jpca.0c00257
J. Phys. Chem. A 2020, 124, 2046−2056

Table 6. Structural Parameters (Å and Degrees) in $(H_3N)_3\cdots ZF_3$ at the MP2/aug-cc-pVDZ Level of Theory

	r(N···Z)	R(Z−F)	Φ(N···Z−F)	Σ(F−Z−F)	ΔΣ(F−Z−F)
$(NH_3)_3\cdots PF_3$	2.959	1.657	163.5	282.0	−9.2
	2.954	1.656	163.4		
	2.949	1.656	163.2		
$(NH_3)_3\cdots AsF_3$	2.822	1.786	159.6	275.1	−13.1
	2.820	1.786	159.6		
	2.820	1.785	159.5		
$(NH_3)_3\cdots SbF_3$	2.789	1.970	150.8	266.5	−18.0
	2.789	1.970	150.7		
	2.788	1.970	150.7		
$(NH_3)_3\cdots BiF_3$	2.769	2.081	150.9	268.3	−18.3
	2.769	2.081	150.9		
	2.769	2.081	150.9		

Table 7. Binding (E_b) and Interaction Energies (E_{int}) (kcal/mol) of ZF_3 Complexes with Three NH_3, Calculated at the MP2/aug-cc-pVDZ (I) and CCSD(T)/aug-cc-pVDZ (II) Levels of Theory[a]

	E_b		E_{int}	
	(I)	(II)	(I)	(II)
		$(H_3N)_3\cdots ZF_3$		
$(NH_3)_3\cdots PF_3$	−10.14	−10.32	−11.86	−11.90
$(NH_3)_3\cdots AsF_3$	−17.39	−17.17	−20.64	−20.30
$(NH_3)_3\cdots SbF_3$	−27.15	−26.50	−34.68	−31.50
$(NH_3)_3\cdots BiF_3$	−34.43	−33.92	−40.24	−39.63

[a]All values corrected for BSSE.

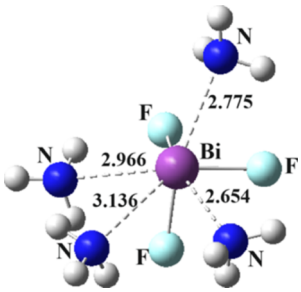

Figure 5. Optimized geometry of $(H_3N)_4\cdots BiF_3$. Distances in Å.

distance which was taken as evidence of a ZB was the sum of the vdW radii.

The data extracted from this survey are presented in Table 8 where each row refers to the number of systems where the indicated number of Z···N pnicogen bonds are present. Taking the first row as an example, there were 7 systems observed where a single pnicogen bond is observed for ZX_3 complexes for which the R(Z···N) distance is at least 110% of the sum of the Z and N covalent bond radii. As the internuclear distance threshold is stretched to 120% and then 130% of this radius sum, the number of such systems is reduced progressively to 5 and then to only 1. Moving down the columns, the number of systems containing two Z···N pnicogen bonds changes to 12, 4, and 4 and then diminishes further to 4, 2, and 1 for the case of three ZBs. It is interesting that there are 9 systems containing four bonds, but this is only true for the very short R(Z···N) contact barely larger than the covalent radii sum, so likely represents a series of slightly stretched covalent bonds.

Relaxation of the restriction of ZX_3 central units to a broader ZR_3, where R can be any substituent of course enlarges the number of such systems observed. The same 110, 120, 130% sequence leads to the rapidly reducing number of 285, 105, and 14 observed single pnicogen bonds. These numbers drop quickly for double and then triple interactions. Again one sees several cases where the 110% threshold would indicate 4 or even 5 pnicogen bonds but none for the more reasonable noncovalent criterion of 120 or 130%. So, while there are certainly numerous systems where a trivalent pnicogen atom engages in 1 or 2 ZBs, this number drops for $n = 3$. It is questionable as to whether there are any systems containing more than 3 ZBs. Figure S6 illustrates a representative sample of just several of the structures captured from the CSD database.[82−89]

Of course, it should be emphasized that the calculations described above pertain to each system in isolation, that is, in vacuo. The crystal structures include effects of neighboring molecules that may modify some of the geometric aspects of each system. So, a reader is cautioned against making precise comparisons.

Table 8. Number of Instances Observed in CSD for Complexes Containing Indicated Number of Z···N Pnicogen Bonds to Central Z Atom[a]

	ZX_3			ZR_3		
number of Z···N contacts	110%	120%	130%	110%	120%	130%
1	7	5	1	285	105	14
2	12	4	4	178	69	7
3	4	2	1[b]	55	36	10[c]
4	9	0	0	12	0	0
5	0	0	0	13	0	0

[a]X refers to halogen atoms, and R refers to any substituent. Percentages indicate the internuclear Z···N distance as a fraction of the sum of their covalent radii. [b]R(Bi···N) = 2.92 Å, 134% of covalent radii sum. [c]1 with Z = P, 0 with As, 7 with Sb, 2 with Bi.

DISCUSSION AND CONCLUSIONS

It appears, then, that the number of pnicogen bonds in which a ZF_3 molecule is capable of engaging is dependent upon the nature of the base. The sp hybridization of N in NCH makes it a fairly weak nucleophile. This N can only approach the Z atom to within about 3 Å, and its binding energy reaches a maximum of 7 kcal/mol for Z = Bi. ZF_3 can engage in two ZBs with NCH, but a third such base engages only weakly with the $(HCN)_2\cdots ZF_3$ and not via a ZB. Its negative charge makes CN^- a powerful nucleophile, binding to ZF_3 by upwards of 20 kcal/mol, as much as 40 kcal/mol for Z = Bi. However, once

https://dx.doi.org/10.1021/acs.jpca.0c00257
J. Phys. Chem. A 2020, 124, 2046−2056

bound to the Lewis acid, the ensuing $NC^-\cdots ZF_3$ complex acquires a negative charge which impedes the approach of a second CN^-. Consequently, the second ZB is very weak and only exists at all for the larger Sb and Bi atoms. A base like NH_3, on the other hand, fits into the Goldilocks region of being just right. Its electrical neutrality prevents the acquisition of charge, so there is no Coulombic obstacle to the approach of multiple NH_3 units. It is a strong base, which can approach to within 2.6−2.8 Å of the central Z atom, and is bound by 4−13 kcal/mol, depending on the size of Z. It is thus able to easily engage simultaneously in three ZBs with ZF_3, with an overall complexation energy of 10−34 kcal/mol. A fourth such bond is marginal though. In the first place, it is only the largest Z = Bi that can engage with four NH_3 units. In addition, the entire complex is held together not only by four ZBs but also by a number of secondary interactions. Moreover, the complexation energy of the $(NH_3)_4\cdots BiF_3$ system is only slightly larger than the smaller $(NH_3)_3\cdots BiF_3$.

Given the strength of the interaction between CN^- and the central Z atom, it is worth considering whether the addition of this anion to a ZF_3 molecule that is already engaged in a pair of ZBs with two HCN molecules might induce the system to engage in a third ZB. This idea seemed plausible as the incoming CN^- will not be repelled by a $(HCN)_2\cdots ZF_3$ complex that already contains a single or double negative charge. In order to examine this possibility, the CN^- anion was initially placed in a wide range of positions with respect to each $(HCN)_2\cdots ZF_3$ complex. Ensuing geometry optimizations led to a variety of situations. For example, in most cases, the anion replaced one of the two HCN units, leaving only two ZBs. In other cases, one or both of the two HCN molecules engaged in a HB with the CN^- anion, or with the F atoms, instead of a ZB with the central ZF_3. However, most importantly, in no case did any of the myriad of initial structures considered optimize to the one containing three ZBs. This result confirms the idea that a third ZB requires a neutral strong base like NH_3.

A prior paper[90] yielded results that have some relevance to the calculations reported above. While the first four N_2 or NCH Lewis bases attach themselves to a central NH_4^+ cation via NH···N H-bonds, succeeding base molecules engage via a N···N pnicogen bond.

Aside from the survey of crystal structures described above, there is additional specific experimental verification of some of these ideas. The Cozzolino group[91] has constructed alkoxide cages containing two Sb···O ZBs, each of which is stronger than 7 kcal/mol. The central Sb atom of $SbCl_3$ engages in three Sb···O contacts short enough to be characterized as ZBs[92] or in three Sb···S bonds with trithiane;[93] three Bi···S bonds with BiX_3 have also been observed quite recently.[94] Radha et al.[95] have shown that a Sb atom can engage in three Sb···S ZBs, that complement its three covalent Sb−S bonds. Their analysis also concluded that a bulky alkyl substituent can inhibit the formation of this number of noncovalent interactions. A very recent work[96] offers further confirmation that with proper formulation of substituents, Bi is capable of three simultaneous ZBs.

The forgoing analysis provides a framework for consideration of multiple pnicogen bonds to a given system, a set of general rules that might be applied to a particular case. As the strength of the base increases, so too does the probability of multiple pnicogen bonds. So, a weak base like NCH might be limited to only two such bonds, whereas a stronger base like NH_3 can engage in three and even four in certain circumstances. In addition, a larger central pnicogen atom is more prone to a greater number of ligands. However, there are secondary issues which might affect these numbers. The overall structural restraints within a crystal, for example, might prevent the central Lewis acid molecule from properly distorting so as to receive a third or fourth ligand. Or the ligands might be large enough that steric repulsions could obstruct the approach of one or more ligands. Another factor is related to the nature of the substituents on the pnicogen atom. The work described above made use of three F substituents which are highly electron-withdrawing and thus enhance the σ-holes that attract the ligands. Less electronegative substituents might be expected to weaken the pnicogen bonds and act to reduce their number. On the other hand, stabilizing interactions between the ligands themselves can promote the ability of the central Z atom to accommodate a larger number of them. The various attractive interactions between the various NH_3 molecules in $F_3Bi(NH_3)_4$ described above is a case in point. Another example of a special circumstance arises if several of the electron donor atoms are part of a single ligand. Such a situation has been observed wherein $SbCl_3$ can be induced to engage in as many as five ZBs when all five electron donor O atoms are part of a single crown ether ligand.[97] While an anion represents a much stronger nucleophile, its charge works against multiple bonding of this type, as was noted above for CN^- because each such anion adds to the electrostatic repulsion between central unit and approaching ligand.

■ ASSOCIATED CONTENT

Supporting Information

The Supporting Information is available free of charge at https://pubs.acs.org/doi/10.1021/acs.jpca.0c00257.

Structural parameters of isolated monomers, deformation energies, AIM descriptors of the neutral and anionic complexes, electronic and Gibbs free energy differences, $V_{s,max}$ of dimers, energies of cooperativity, AIM descriptors of the neutral and anionic trimers, $V_{s,max}$ of trimers, AIM descriptors of the tetramers, crystal structures of tetra and penta-coordinated complexes (from CSD); and Structural parameters in isolated ZF_3 (Z = P, As, Sb, Bi) calculated at the MP2/aug-cc-pVDZ level of theory (PDF)

■ AUTHOR INFORMATION

Corresponding Authors

Rafał Wysokiński − *Faculty of Chemistry, Wrocław University of Science and Technology, 50-370 Wrocław, Poland;* orcid.org/0000-0002-1133-3535; Email: rafal.wysokinski@pwr.edu.pl

Steve Scheiner − *Department of Chemistry and Biochemistry, Utah State University, Logan, Utah 84322-0300, United States;* orcid.org/0000-0003-0793-0369; Email: steve.scheiner@usu.edu

Authors

Wiktor Zierkiewicz − *Faculty of Chemistry, Wrocław University of Science and Technology, 50-370 Wrocław, Poland;* orcid.org/0000-0002-4038-5959

Mariusz Michalczyk − *Faculty of Chemistry, Wrocław University of Science and Technology, 50-370 Wrocław, Poland;* orcid.org/0000-0002-6495-6963

Complete contact information is available at:

https://pubs.acs.org/10.1021/acs.jpca.0c00257

Notes

The authors declare no competing financial interest.

■ ACKNOWLEDGMENTS

This work was financed in part by a statutory activity subsidy from the Polish Ministry of Science and Higher Education for the Faculty of Chemistry of Wroclaw University of Science and Technology. A generous allotment of computer time from the Wroclaw Supercomputer and Networking Center is acknowledged.

■ REFERENCES

(1) Kendall, K.; Roberts, A. D. van der Waals forces influencing adhesion of cells. *Philos. Trans. R. Soc. London, Ser. B* **2015**, *370*, 20140078.
(2) Müller-Dethlefs, K.; Hobza, P. Noncovalent Interactions: A Challenge for Experiment and Theory. *Chem. Rev.* **2000**, *100*, 143−168.
(3) Grabowski, S. *Hydrogen Bonding—New Insights*, 1 ed.; Springer Netherlands: Berlin, 2006; Vol. *3*, p 524.
(4) Desiraju, G. R.; Steiner, T. *The Weak Hydrogen Bond: In Structural Chemistry and Biology*; Oxford University Press: Oxford, 2001.
(5) Gilli, G.; Gilli, P. The Strength of the H-Bond: Definitions and Thermodynamics. *The Nature of the Hydrogen Bond*; Oxford, 2009; pp 222−244.
(6) Zundel, G.; Sandorfy, C.; Schuster, P. *The Hydrogen Bond: Recent Developments in Theory and Experiments*; North-Holland: Amsterdam, Oxford, 1976; Vol. *2*.
(7) Gilli, G.; Gilli, P. *The Nature of the Hydrogen Bond: Outline of a Comprehensive Hydrogen Bond Theory*; Oxford University Press: Oxford, 2013.
(8) Scheiner, S. *Hydrogen Bonding: A Theoretical Perspective*; Oxford University Press, 1997.
(9) Politzer, P.; Murray, J. S.; Concha, M. C. σ-hole bonding between like atoms; a fallacy of atomic charges. *J. Mol. Model.* **2008**, *14*, 659−665.
(10) Murray, J. S.; Politzer, P. The electrostatic potential: an overview. *Wiley Interdiscip. Rev.: Comput. Mol. Sci.* **2011**, *1*, 153−163.
(11) Murray, J. S.; Lane, P.; Clark, T.; Riley, K. E.; Politzer, P. σ-Holes, π-holes and electrostatically-driven interactions. *J. Mol. Model.* **2012**, *18*, 541−548.
(12) Aakeröy, C. B.; Alavi, S.; Brammer, L.; Bryce, D. L.; Clark, T.; Del Bene, J. E.; Edwards, A. J.; Esterhuysen, C.; Guru Row, T. N.; Kennepohl, P.; et al. Computational approaches and sigma-hole interactions: general discussion. *Faraday Discuss.* **2017**, *203*, 131−163.
(13) Murray, J. S.; Politzer, P. Molecular electrostatic potentials and noncovalent interactions. *Wiley Interdiscip. Rev.: Comput. Mol. Sci.* **2017**, *7*, No. e1326.
(14) Politzer, P.; Murray, J. S. σ-Hole Interactions: Perspectives and Misconceptions. *Crystals* **2017**, *7*, 212.
(15) Politzer, P.; Murray, J. S.; Clark, T.; Resnati, G. The σ-hole revisited. *Phys. Chem. Chem. Phys.* **2017**, *19*, 32166−32178.
(16) Politzer, P.; Murray, J. S. Analysis of Halogen and Other σ-Hole Bonds in Crystals. *Crystals* **2018**, *8*, 42.
(17) Politzer, P.; Murray, J. S. Halogen Bonding: An Interim Discussion. *Chemphyschem* **2013**, *14*, 278−294.
(18) Wang, H.; Wang, W.; Jin, W. J. σ-Hole Bond vs π-Hole Bond: A Comparison Based on Halogen Bond. *Chem. Rev.* **2016**, *116*, 5072−5104.
(19) Bulfield, D.; Huber, S. M. Halogen Bonding in Organic Synthesis and Organocatalysis. *Chem.—Eur. J.* **2016**, *22*, 14434−14450.
(20) Cordier, P.; Tournilhac, F.; Soulié-Ziakovic, C.; Leibler, L. Self-healing and thermoreversible rubber from supramolecular assembly. *Nature* **2008**, *451*, 977−980.
(21) Hobza, P.; Müller, D. K. *Non-Covalent Interactions*; Royal Society of Chemistry: Cambridge, 2011.
(22) Lacour, J.; Moraleda, D. Chiral anion-mediated asymmetric ion pairing chemistry. *Chem. Commun.* **2009**, 7073−7089.
(23) Lehn, J.-M. Toward Self-Organization and Complex Matter. *Science* **2002**, *295*, 2400.
(24) Lim, J. Y. C.; Beer, P. D. Sigma-Hole Interactions in Anion Recognition. *Chem* **2018**, *4*, 731−783.
(25) Strekowski, L.; Wilson, B. Noncovalent interactions with DNA: an overview. *Mutat. Res.* **2007**, *623*, 3−13.
(26) Stupp, S. I.; LeBonheur, V.; Walker, K.; Li, L. S.; Huggins, K. E.; Keser, M.; Amstutz, A. Supramolecular Materials: Self-Organized Nanostructures. *Science* **1997**, *276*, 384.
(27) Wagner, J. P.; Schreiner, P. R. London Dispersion in Molecular Chemistry-Reconsidering Steric Effects. *Angew. Chem., Int. Ed.* **2015**, *54*, 12274−12296.
(28) Whitesides, G.; Mathias, J.; Seto, C. Molecular self-assembly and nanochemistry: a chemical strategy for the synthesis of nanostructures. *Science* **1991**, *254*, 1312.
(29) Zhao, Y.; Cotelle, Y.; Sakai, N.; Matile, S. Unorthodox Interactions at Work. *J. Am. Chem. Soc.* **2016**, *138*, 4270−4277.
(30) Zhou, P.; Huang, J.; Tian, F. Specific Noncovalent Interactions at Protein-Ligand Interface: Implications for Rational Drug Design. *Curr. Med. Chem.* **2012**, *19*, 226−238.
(31) Michalczyk, M.; Zierkiewicz, W.; Wysokiński, R.; Scheiner, S. Hexacoordinated Tetrel-Bonded Complexes between TF4(T=Si, Ge, Sn, Pb) and NCH: Competition between σ- and π-Holes. *ChemPhysChem* **2019**, *20*, 959−966.
(32) Zierkiewicz, W.; Michalczyk, M.; Wysokiński, R.; Scheiner, S. Dual Geometry Schemes in Tetrel Bonds: Complexes between TF4 (T = Si, Ge, Sn) and Pyridine Derivatives. *Molecules* **2019**, *24*, 376.
(33) Zierkiewicz, W.; Michalczyk, M.; Wysokinski, R.; Scheiner, S. On the ability of pnicogen atoms to engage in both σ and π-hole complexes. Heterodimers of ZF2C6H5 (Z = P, As, Sb, Bi) and NH3. *J. Mol. Model.* **2019**, *25*, 152.
(34) Wysokiński, R.; Michalczyk, M.; Zierkiewicz, W.; Scheiner, S. Influence of monomer deformation on the competition between two types of σ-holes in tetrel bonds. *Phys. Chem. Chem. Phys.* **2019**, *21*, 10336−10346.
(35) Esrafili, M. D.; Vakili, M.; Solimannejad, M. Cooperative effects in pnicogen bonding: (PH2F)2-7 and (PH2Cl)2-7 clusters. *Chem. Phys. Lett.* **2014**, *609*, 37−41.
(36) Adhikari, U.; Scheiner, S. Comparison of P···D (D = P,N) with other noncovalent bonds in molecular aggregates. *J. Chem. Phys.* **2011**, *135*, 184306.
(37) Del Bene, J. E.; Alkorta, I.; Elguero, J. Hydrogen and Halogen Bonding in Cyclic FH(4-n):FCln Complexes, for n = 0-4. *J. Phys. Chem. A* **2018**, *122*, 2587−2597.
(38) Sánchez-Sanz, G.; Trujillo, C. Improvement of Anion Transport Systems by Modulation of Chalcogen Interactions: The influence of solvent. *J. Phys. Chem. A* **2018**, *122*, 1369−1377.
(39) Chakraborty, S.; Maji, S.; Ghosh, R.; Jana, R.; Datta, A.; Ghosh, P. Aryl-platform-based tetrapodal 2-iodo-imidazolium as an excellent halogen bond receptor in aqueous medium. *Chem. Commun.* **2019**, *55*, 1506−1509.
(40) Scheiner, S. Differential Binding of Tetrel-Bonding Bipodal Receptors to Monatomic and Polyatomic Anions. *Molecules* **2019**, *24*, 227.
(41) Lee, L. M.; Tsemperouli, M.; Poblador-Bahamonde, A. I.; Benz, S.; Sakai, N.; Sugihara, K.; Matile, S. Anion Transport with Pnictogen Bonds in Direct Comparison with Chalcogen and Halogen Bonds. *J. Am. Chem. Soc.* **2019**, *141*, 810−814.
(42) Lim, J. Y. C.; Marques, I.; Félix, V.; Beer, P. D. Chiral halogen and chalcogen bonding receptors for discrimination of stereo- and geometric dicarboxylate isomers in aqueous media. *Chem. Commun.* **2018**, *54*, 10851−10854.

(43) Scheiner, S. Comparison of halide receptors based on H, halogen, chalcogen, pnicogen, and tetrel bonds. *Faraday Discuss.* **2017**, *203*, 213−226.
(44) Semenov, N. A.; Gorbunov, D. E.; Shakhova, M. V.; Salnikov, G. E.; Bagryanskaya, I. Y.; Korolev, V. V.; Beckmann, J.; Gritsan, N. P.; Zibarev, A. V. Donor-Acceptor Complexes between 1,2,5-Chalcogenadiazoles (Te, Se, S) and the Pseudohalides CN− and XCN− (X=O, S, Se, Te). *Chem.—Eur. J.* **2018**, *24*, 12983−12991.
(45) Scheiner, S. Assembly of Effective Halide Receptors from Components. Comparing Hydrogen, Halogen, and Tetrel Bonds. *J. Phys. Chem. A* **2017**, *121*, 3606−3615.
(46) Lim, J. Y. C.; Beer, P. D. A pyrrole-containing cleft-type halogen bonding receptor for oxoanion recognition and sensing in aqueous solvent media. *New J. Chem.* **2018**, *42*, 10472−10475.
(47) Stoesser, J.; Rojas, G.; Bulfield, D.; Hidalgo, P. I.; Pasán, J.; Ruiz-Pérez, C.; Jiménez, C. A.; Huber, S. M. Halogen bonding two-point recognition with terphenyl derivatives. *New J. Chem.* **2018**, *42*, 10476−10480.
(48) Dreger, A.; Engelage, E.; Mallick, B.; Beer, P. D.; Huber, S. M. The role of charge in 1,2,3-triazol(ium)-based halogen bonding activators. *Chem. Commun.* **2018**, *54*, 4013−4016.
(49) Zhou, L.; Lu, Y.; Xu, Z.; Peng, C.; Liu, H. Ion-pair recognition based on halogen bonding: a case of the crown-ether receptor with iodo-trizole moiety. *Struct. Chem.* **2017**, *29*, 533−540.
(50) Scheiner, S. Tetrel Bonding as a Vehicle for Strong and Selective Anion Binding. *Molecules* **2018**, *23*, 1147.
(51) Scheiner, S.; Michalczyk, M.; Zierkiewicz, W. Structures of clusters surrounding ions stabilized by hydrogen, halogen, chalcogen, and pnicogen bonds. *Chem. Phys.* **2019**, *524*, 55−62.
(52) Scheiner, S.; Michalczyk, M.; Wysokiński, R.; Zierkiewicz, W. Structures and energetics of clusters surrounding diatomic anions stabilized by hydrogen, halogen, and other noncovalent bonds. *Chem. Phys.* **2020**, *530*, 110590.
(53) Zierkiewicz, W.; Wysokiński, R.; Michalczyk, M.; Scheiner, S. Chalcogen bonding of two ligands to hypervalent YF4 (Y = S, Se, Te, Po). *Phys. Chem. Chem. Phys.* **2019**, *21*, 20829−20839.
(54) Grabowski, S. J. Coordination of Be and Mg Centres by HCN Ligands - Be...N and Mg...N Interactions. *Chemphyschem* **2018**, *19*, 1830−1840.
(55) Scheiner, S. On the capability of metal-halogen groups to participate in halogen bonds. *Crystengcomm* **2019**, *21*, 2875−2883.
(56) Grabowski, S. J. Tetrel bonds, penta- and hexa-coordinated tin and lead centres. *Appl. Organomet. Chem.* **2017**, *31*, No. e3727.
(57) Aakeroy, C. B.; Bryce, D. L.; Desiraju, G. R.; Frontera, A.; Legon, A. C.; Nicotra, F.; Rissanen, K.; Scheiner, S.; Terraneo, G.; Metrangolo, P.; et al. Definition of the chalcogen bond (IUPAC Recommendations 2019). *Pure Appl. Chem.* **2019**, *91*, 1889−1892.
(58) Desiraju, G. R.; Ho, P. S.; Kloo, L.; Legon, A. C.; Marquardt, R.; Metrangolo, P.; Politzer, P.; Resnati, G.; Rissanen, K. Definition of the halogen bond (IUPAC recommendations 2013). *Pure Appl. Chem.* **2013**, *85*, 1711−1713.
(59) Alkorta, I.; Bene, J.; Elguero, J. The Pnicogen Bond in Review: Structures, Binding Energies, Bonding Properties, and Spin-Spin Coupling Constants of Complexes Stabilized by Pnicogen Bonds. *Noncovalent Forces*; Springer, 2015; pp 191−263.
(60) Møller, C.; Plesset, M. S. Note on an approximation treatment for many-electron systems. *Phys. Rev.* **1934**, *46*, 618−622.
(61) Dunning, T. H. Gaussian basis sets for use in correlated molecular calculations. I. The atoms boron through neon and hydrogen. *J. Chem. Phys.* **1989**, *90*, 1007−1023.
(62) Liu, X.; Cheng, J.; Li, Q.; Li, W. Competition of hydrogen, halogen, and pnicogen bonds in the complexes of HArF with XH2P (X=F, Cl, and Br). *Spectrochim. Acta, Part A* **2013**, *101*, 172−177.
(63) Hauchecorne, D.; Herrebout, W. A. Experimental Characterization of C-X···Y-C (X = Br, I; Y = F, Cl) Halogen-Halogen Bonds. *J. Phys. Chem. A* **2013**, *117*, 11548−11557.
(64) Zhao, Q.; Feng, D. C.; Sun, Y. M.; Hao, J. C.; Cai, Z. T. Theoretical Investigations on the Weak Nonbonded C=S···CH2 Interactions: Chalcogen-Bonded Complexes With Singlet Carbene as an Electron Donor. *Int. J. Quantum Chem.* **2011**, *111*, 3881−3887.
(65) Scheiner, S. Effects of Substituents upon the P···N Noncovalent Interaction: The Limits of Its Strength. *J. Phys. Chem. A* **2011**, *115*, 11202−11209.
(66) Peterson, K. A. Systematically convergent basis sets with relativistic pseudopotentials. I. Correlation consistent basis sets for the post-d group 13-15 elements. *J. Chem. Phys.* **2003**, *119*, 11099−11112.
(67) Purvis, G. D.; Bartlett, R. J. A full coupled-cluster singles and doubles model: The inclusion of disconnected triples. *J. Chem. Phys.* **1982**, *76*, 1910−1918.
(68) Pople, J. A.; Head-Gordon, M.; Raghavachari, K. Quadratic configuration interaction. A general technique for determining electron correlation energies. *J. Chem. Phys.* **1987**, *87*, 5968−5975.
(69) Lee, C.; Yang, W.; Parr, R. G. Development of the Colle-Salvetti correlation-energy formula into a functional of the electron density. *Phys. Rev. B: Condens. Matter Mater. Phys.* **1988**, *37*, 785−789.
(70) Raghavachari, K.; Trucks, G. W.; Pople, J. A.; Head-Gordon, M. A fifth-order perturbation comparison of electron correlation theories. *Chem. Phys. Lett.* **1989**, *157*, 479−483.
(71) Becke, A. D. Density-functional thermochemistry. III. The role of exact exchange. *J. Chem. Phys.* **1993**, *98*, 5648−5652.
(72) Weigend, F.; Ahlrichs, R. Balanced basis sets of split valence, triple zeta valence and quadruple zeta valence quality for H to Rn: Design and assessment of accuracy. *Phys. Chem. Chem. Phys.* **2005**, *7*, 3297−3305.
(73) Weigend, F. Accurate Coulomb-fitting basis sets for H to Rn. *Phys. Chem. Chem. Phys.* **2006**, *8*, 1057.
(74) Boys, S. F.; Bernardi, F. The calculation of small molecular interactions by the differences of separate total energies. Some procedures with reduced errors. *Mol. Phys.* **1970**, *19*, 553−566.
(75) Frisch, M. J.; Trucks, G. W.; Schlegel, H. B.; Scuseria, G. E.; Robb, M. A.; Cheeseman, J. R.; Scalmani, G.; Barone, V.; Petersson, G. A.; Nakatsuji, H.; et al. *Gaussian 16*, Rev. C.01: Wallingford, CT, 2016.
(76) Bulat, F. A.; Toro-Labbé, A.; Brinck, T.; Murray, J. S.; Politzer, P. Quantitative analysis of molecular surfaces: areas, volumes, electrostatic potentials and average local ionization energies. *J. Mol. Model.* **2010**, *16*, 1679−1691.
(77) Lu, T.; Chen, F. Multiwfn: a multifunctional wavefunction analyzer. *J. Comput. Chem.* **2012**, *33*, 580−592.
(78) Lu, T.; Chen, F. Quantitative analysis of molecular surface based on improved Marching Tetrahedra algorithm. *J. Mol. Graphics Modell.* **2012**, *38*, 314−323.
(79) Keith, A. T. *AIMAll*, version 14.11.23; TK Gristmill Software: Overland Park KS, USA, 2014, aim.tkgristmill.com.
(80) Glendening, E. D.; Landis, C. R.; Weinhold, F. NBO 6.0: natural bond orbital analysis program. *J. Comput. Chem.* **2013**, *34*, 1429−1437.
(81) Groom, C. R.; Bruno, I. J.; Lightfoot, M. P.; Ward, S. C. The Cambridge Structural Database. *Acta Crystallogr., Sect. B: Struct. Sci., Cryst. Eng. Mater.* **2016**, *72*, 171−179.
(82) Webster, M.; Keats, S. Crystal Structure of Arsenic Trichloride-Trimethylamine, Asci3,Nm3. *J. Chem. Soc. A* **1971**, *6*, 836−838.
(83) Müller, G.; Brand, J.; Jetter, S. E. Donor-acceptor complexes between organoamines and phosphorus tribromide. *Z. Naturforsch., B: J. Chem. Sci.* **2001**, *56*, 1163−1171.
(84) Burford, N.; Edelstein, E.; Landry, J. C.; Ferguson, M. J.; McDonald, R. Identification of new N-Sb topologies: understanding the sequential dehydrochloride coupling of primary amines and trichloropnictines. *Chem. Commun.* **2005**, 5074−5076.
(85) Mourgas, G.; Nieger, M.; Förster, D.; Gudat, D. Conformationally Constrained N-Heterocyclic Phosphine-Diimine with Dual Functionality. *Inorg. Chem.* **2013**, *52*, 4104−4112.
(86) Day, B. M.; Coles, M. P.; Hitchcock, P. B. Neutral and Anionic Antimony(III) Species Supported by a Bicyclic Guanidinate. *Eur. J. Inorg. Chem.* **2012**, 841−846.

https://dx.doi.org/10.1021/acs.jpca.0c00257
J. Phys. Chem. A 2020, 124, 2046−2056

(87) Bell, S. A.; Geib, S. J.; Meyer, T. Y. Iminophosphorane-mediated carbodiimide metathesis. *Chem. Commun.* **2000**, 1375−1376.
(88) Davidovich, R. L.; Tkachev, V. V.; Atovmyan, L. O. Crystal-Structure of Molecular Adduct of Antimony(Iii) Fluoride with Nicotinamide Sbf3-Center-Dot-2l. *Koord. Khim.* **1995**, *21*, 20−22.
(89) Alič, B.; Štefančič, A.; Tavčar, G. Small molecule activation: SbF3 auto-ionization supported by transfer and mesoionic NHC rearrangement. *Dalton Trans.* **2017**, *46*, 3338−3346.
(90) Grabowski, S. J. Clusters of Ammonium Cation-Hydrogen Bond versus σ-Hole Bond. *Chemphyschem* **2014**, *15*, 876−884.
(91) Moaven, S.; Yu, J.; Yasin, J.; Unruh, D. K.; Cozzolino, A. F. Precise Steric Control over 2D versus 3D Self-Assembly of Antimony(III) Alkoxide Cages through Strong Secondary Bonding Interactions. *Inorg. Chem.* **2017**, *56*, 8372−8380.
(92) Alcock, N. W.; Ravindran, M.; Roe, S. M.; Willey, G. R. Synthesis and Structure of Antimony(Iii)Chloride-1,4,7,10,13,16-Hexaoxocyclooctadecane-(18-Crown-6)-Acetonitrile (1/1/1). *Inorg. Chim. Acta* **1990**, *167*, 115−118.
(93) Leroy, C.; Johannson, R.; Bryce, D. L. 121/123Sb Nuclear Quadrupole Resonance Spectroscopy: Characterization of Non-Covalent Pnictogen Bonds and NQR Crystallography. *J. Phys. Chem. A* **2019**, *123*, 1030−1043.
(94) Mokrai, R.; Barrett, J.; Apperley, D. C.; Batsanov, A. S.; Benkő, Z.; Heift, D. Weak Pnictogen Bond with Bismuth: Experimental Evidence Based on Bi−P Through-Space Coupling. *Chem.—Eur. J.* **2019**, *25*, 4017−4024.
(95) Radha, A.; Kumar, S.; Sharma, D.; Jassal, A. K.; Zaręba, J. K.; Franconetti, A.; Frontera, A.; Sood, P.; Pandey, S. K. ···Indirect influence of alkyl substituent on sigma-hole interactions: The case study of antimony(III) diphenyldithiophosphates with covalent Sb-S and non-covalent Sb···S pnictogen bonds. *Polyhedron* **2019**, *173*, 114126.
(96) Moaven, S.; Andrews, M. C.; Polaske, T. J.; Karl, B. M.; Unruh, D. K.; Bosch, E.; Bowling, N. P.; Cozzolino, A. F. Triple-Pnictogen Bonding as a Tool for Supramolecular Assembly. *Inorg. Chem.* **2019**, *58*, 16227−16235.
(97) Hough, E.; Nicholson, D. G.; Vasudevan, A. K. Stereochemical role of lone pairs in main-group elements. Part 3. Structure and bonding in trichloro(1,4,7,10,13-pentaoxacyclopentadecane)-antimony(III) studied by means of X-ray crystallography at 120 K. *J. Chem. Soc., Dalton Trans.* **1987**, 427−430.

https://dx.doi.org/10.1021/acs.jpca.0c00257
J. Phys. Chem. A 2020, 124, 2046−2056